Advances in Nano Research, *Vol. 14, No. 2 (2023) 117-126*
https://doi.org/10.12989/anr.2023.14.2.117

Optimization of FSW of Nano-silica-reinforced ABS T-Joint using a Box-Behnken Design (BBD)

Mahyar Motamedi Kouchaksarai and Yasser Rostamiyan*

Department of mechanical engineering, Sari branch, Islamic Azad University, Sari, Iran

(*Received October 31, 2022, Revised September 18, 2022, Accepted October 31, 2022*)

Abstract. This experimental study investigated friction stir welding (FSW) of the acrylonitrile-butadiene-styrene (ABS) T-joint in the presence of various nano-silica levels. This study aim to handle the drawbacks of the friction stir welding (FSW) of an ABS T-joint with various quantity of nanoparticles and assess the performance of nanoparticles in the welded joint. Moreover, the relationship between the nanoparticle quantity and FSW was analyzed using response surface methodology (RSM) Box–Behnken design. The input parameters were the tool rotation speed (400, 600, 800 rpm), the transverse speed (20, 30, 40 mm/min), and the nano-silica level (0.8, 1.6, 2.4 g). The tensile strength of the prepared specimens was determined by the universal testing machine. Silica nanoparticles were used to improve the mechanical properties (the tensile strength) of ABS and investigate the effect of various FSW parameters on the ABS T-joint. The results of Box-Behnken RSM revealed that sound joints with desired characteristics and efficiency are fabricated at tool rotation speed 755 rpm, transverse speed 20 mm/min, and nano-silica level 2.4 g. The scanning electron microscope (SEM) images revealed the crucial role of silica nanoparticles in reinforcing the ABS T-joint. The SEM images also indicated a decrease in the nanoparticle size by the tool rotation, leading to the filling and improvement of seams formed during FSW of the ABS T-joint.
Keywords: ABS; friction stir welding; nano-silica; optimization; SEM

1. Introduction

Most automotive parts are currently produced from polymeric materials, in particular thermoplastics. The use of plastics instead of metals makes the production of automotive parts easier and cheaper. The facile processing of plastics in comparison with metals provides a variety of design alternatives. Friction stir welding (FSW) is a nonhazardous eco-friendly process. Due to the flexibility of FSW in the design and construction of heterogeneous structures, this type of welding is extensively used in modern industries. In general, polymer joints can be welded by (1) heat transfer, (2) thermal radiation, and (3) mechanical friction joint welding. Toxic gases released during welding in the first and second processes are harmful to humans and the environment (Zoltán Kiss *et al*. 2007). Friction stir welding consists of three main steps. In the first stage, as the tool rotates at the welding site, the solid materials of the joint assume a semi-molten form. In the second stage, the semi-molten materials are mixed while the welding tool is displaced along the weld line. In the third stage, materials are rapidly cooled down to the ambient temperature after the removal of the welding tool, leading to the joining of parts (Peng *et al*. 2018). In friction stir welding, the tool rotation and the resulting friction with the workpiece generate heat, causing a decrease in the joint strength and increasing the ductility (formability) of materials around the pin. The transitional motion also causes the displacement of materials from the front to the back of the tool and joining. This indicates the significant role of heat transfer in the FSW process. On the other hand, the tool rotation speed, the transverse speed, the tool geometry, etc. play a key role in controlling the input heat and thereby the disturbance of the flow regime, microstructure development, and ultimately the resulting weld quality.

Kiss *et al*. studied the effect of tool rotation speed and transverse speed on the mechanical and structural properties of PE sheet welding. The effect of the groove torsional angle was also investigated. According to their results, higher tensile strength and better crystalline structure were obtained by decreasing the transverse speed and increasing the tool rotation speed and torsional angle (Kiss *et al*. 2012). Razgoei *et al*. investigated the effect of tool rotation speed, transverse speed, dwell time, and pin diameter on the high-density polyethylene (HDPE) specimens by Taguchi experimental design. A fixed scratching surface with low thermal conductivity was used instead of the tool shoulder to reduce the cooling time of welded parts and achieve a uniform heat distribution in the welding zone (Rezgui *et al*. 2010). Saeedi *et al*. studied the effect of tool rotation speed, transverse speed, and FSW tool geometry on the mechanical and structural properties of PP sheet welds. According to their results, the mechanical properties of PP welds were improved by increasing the tool rotation speed. The tool geometry had a significant role in the brittleness of specimens so that the specimens welded by the grooved tool showed less brittleness than those welded by the stud tool (Saeedy *et al*. 2010). Anna *et al*. studied friction stir welding of PE sheets. The effects of tool rotation speed, transverse speed, tool diameter, and two heating methods,

*Corresponding author, Associate Professor,
E-mail: yasser.rostamiyan@iausari.ac.ir
[a] M.Sc., Email: Mahyarmotamedi.k@gmail.com

ISSN: 2287-237X (Print), 2287-2388 (Online)

namely heating by a hairdryer and a hot plate, were investigated on the mechanical and structural properties of specimens by differential scanning calorimetry (DSC) (Squeo *et al*. 2009). Chang *et al*. investigated the effect of carbon nanotubes (CNTs) and various parameters on the friction stir welding of HDPE and ABS. Their results showed a significant reduction in the number of defects such as cracks and pinholes in the specimens in the presence of nanoparticles (Gao *et al*. 2015). Sadeghian *et al*. optimized the FSW parameters of ABS by experimental design. According to their results, the conical pin, a tool speed rotation of 900 rpm, a transverse speed of 20 mm/min, and a tool angle of 2° were found as the optimal FSW parameters (Sadeghian *et al*. 2015). Azhiri *et al*. studied friction stir welding of ABS joints by adding various nano-silica levels. The effect of the reciprocating movement of the rotational welding tool on the microstructure and tensile strength of the specimen was investigated by scanning electron microscopy (SEM) (Azhiri *et al*. 2018). Santosh *et al*. investigated on the friction stir butt welding. The result found to be highly feasible to join polycarbonate sheets with adequate joint efficiency by appropriate selection of welding parameter settings, also the weld quality was poor at low tool rotational speed with high welding speed because of insufficient weld heat input (Sahu *et al*. 2020). Ming *et al*. found that tool tilt angle plays an effective role in generating heat at welding zone, the result showed that with a 2.5◦ tool tilt angle, the heat generation at tool/workpiece interface plays a more important role due to the forging effect of tilted tool (Zhai *et al*. 2020). So generaly with a tool tilt angle of 2.5◦, temperature at points of tool/ workpiece interface is higher than that in case of 0◦ tool tilt angle.

According to the literature on polymer welding, the optimal ranges for FSW parameters are as follows: the transverse speed of 10 to 25 mm/min and the tool rotation speed of 500 to 900 rpm (Sahu *et al*. 2018). A wider transverse speed range is used in this study than that used in the literature. By adding nano-silica at the joint zone, a relatively high-strength joint can be achieved even at a transverse speed of 30 mm/min. The effect of input parameters on the results was analyzed with the Minitab software.

The response surface methodology (RSM) is a statistical and mathematical technique to develop, improve, and optimize processes (Mäkelä 2017). A process can be defined as a mechanism of converting a set of inputs into a set of outputs, known as response variables. RSM estimates the relationship(s) between one or more response variables and a number of independent variables through a set of designed tests and regression analysis (Rahimipetroudi *et al*. 2020). The RSM consists of a number of steps, namely (1) two-factor tests to screen the influential input variables, (2) regression analysis to obtain the fitness function of outputs based on the inputs, and (3) optimization to find the optimal levels of the input variables (Myers *et al*.2016).

The rotation tool in the FSW of T-joints should be gently driven into the workpiece to reach the T-joint flange, and cavities are likely to appear in the weld. This study employed nanoparticles in the weld to investigate their contribution to handling this obstacle. Moreover, the direct effects of FSW parameters and nanoparticles, which are associated, were analyzed using the Box–Behnken design of the response surface methodology (RSM). The use of nanoparticles in the T-joint in friction stir welding (FSW) and the performance evaluation of nanoparticles are the novelties of the present work.

Table 1 Properties of ABS material

Tensile Strength (Mpa)	Hardness (HV)	Thermal expansion coefficient (m/mK)	Melt Point (˚C)	Density (kg/m^3)
43	11	73.8×10^{-6}	160	905

2. Materials and methods

As a thermoplastic polymer, acrylonitrile-butadiene-styrene (ABS) with a glass transition temperature (Tg) of 105°C was used in the study. The properties of ABS are summarized in Table 1. The 150 mm×100 mm ABS sheets with thicknesses of 4 and 10 mm were prepared. The ABS sheet was predetermined dimensions with the laser cutting. The 4- and 10-mm thick sheets were, respectively, used as the upper sheet of the T-joint and that perpendicular to the upper sheet. According to the specimen dimensions, a fixture was designed and constructed to fix the ABS T-joint during welding Fig. 1(a).

The FSW tool for ABS welding was constructed of AISI H13 steel Fig. 1(b). A constant tool tilt angle of 1.5° (Zhai *et al.* 2020) and a plunge depth of 0.5 mm were considered in this study. The rotational tool with a shoulder diameter of 18 mm, a pin diameter of 5 mm, and a length of 7 mm was used in the FSW process. Both pure (without nano-silica) and nano-silica-reinforced specimens were prepared, and three FSW parameters, each at three levels, including the tool rotation speed (400, 600, 800 rpm), transverse speed (20, 30, 40 mm/min), and nano-silica level (0.8, 1.6, 2.4 g) were investigated. A 0.5-mm thick groove with depths of 1, 2, and 3 mm was created on the face of the 10-mm thick sheets prepared for friction stir welding and filled with nano-silica powder. The grooves with different depths were filled with different nano-silica levels. The upper sheet was then placed on the desired face and the FSW process was performed along the grooves. To achieve optimal values, the effects of the tool rotation speed and the transverse speed on the mechanical properties of the ABS T-joint and nano-silica reinforcement were investigated by the 3-factor Box–Behnken experimental design. The results were analyzed with Minitab software (version 18.1.). A total of 15 experiments, shown in Table 2, were considered.

The milling machine (4301, Tabriz) was used for friction stir welding. The universal testing machine (SANTAM, Iran) was employed in the tensile strength testing. The 4-mm thick polymer sheet was fixed on the fixture support, and the 10-mm thick T-flange was connected to the upper movable grip of the universal machine Fig. 1(c). Field scanning electron microscopy (FE-SEM, FEI NOVA NanoSEM 450) was used to identify the dispersion of silica nanoparticles at the welding area. Three welding specimens were tested by the universal testing machine

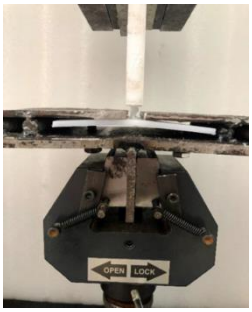

(c)

(b)

(a)

Fig. 1 (a) Experimental setup including FSW attachment on a milling machine, clamping system, (b) FSW tool, (c) specimens of t-joint after the tensile test

Table 2 Box–Behnken design matrix containing 15 experimental runs and tensile force of nanosilica-reinforced

Run order	Tool rotation Speed (rpm)	Transverse Speed (mm/min)	Nano-silica (g)	Tensile Force (N)
1	600	30	1.6	1352.0
2	600	40	2.4	1301.9
3	400	20	1.6	941.0
4	600	20	0.8	1400.2
5	600	30	1.6	1256.2
6	400	30	0.8	870.0
7	600	20	2.4	1459.0
8	800	30	0.8	1164.0
9	400	30	2.4	918.0
10	600	40	0.8	1266.0
11	800	20	1.6	1474.2
12	800	40	1.6	1216.0
13	600	30	1.6	1335.8
14	400	40	1.6	815.0
15	800	30	2.4	1601.4

Table 3 Tensile strength pure specimens

Run order	Tool rotation Speed (rpm)	Transverse Speed (mm/min)	Tensile Force (N)
1	400	20	812.5
2	400	30	628.4
3	400	40	501.7
4	600	20	1234.8
5	600	30	986.2
6	600	40	722.4
7	800	20	1307.1
8	800	30	1050.3
9	800	40	866.3

for each design experiment, and the average strength was calculated.

3. Results and discussion

Tables 2-3 list the tensile strength of nano-silica-reinforced and pure specimens, respectively. The tensile strength determined based on the ultimate load was used in the analyses.

3.1 Nanosilica-reinforced specimens at a constant tool rotation speed

Fig. 2(a) compares the reinforced specimens at the constant tool rotation speed of 400 rpm. The specimen

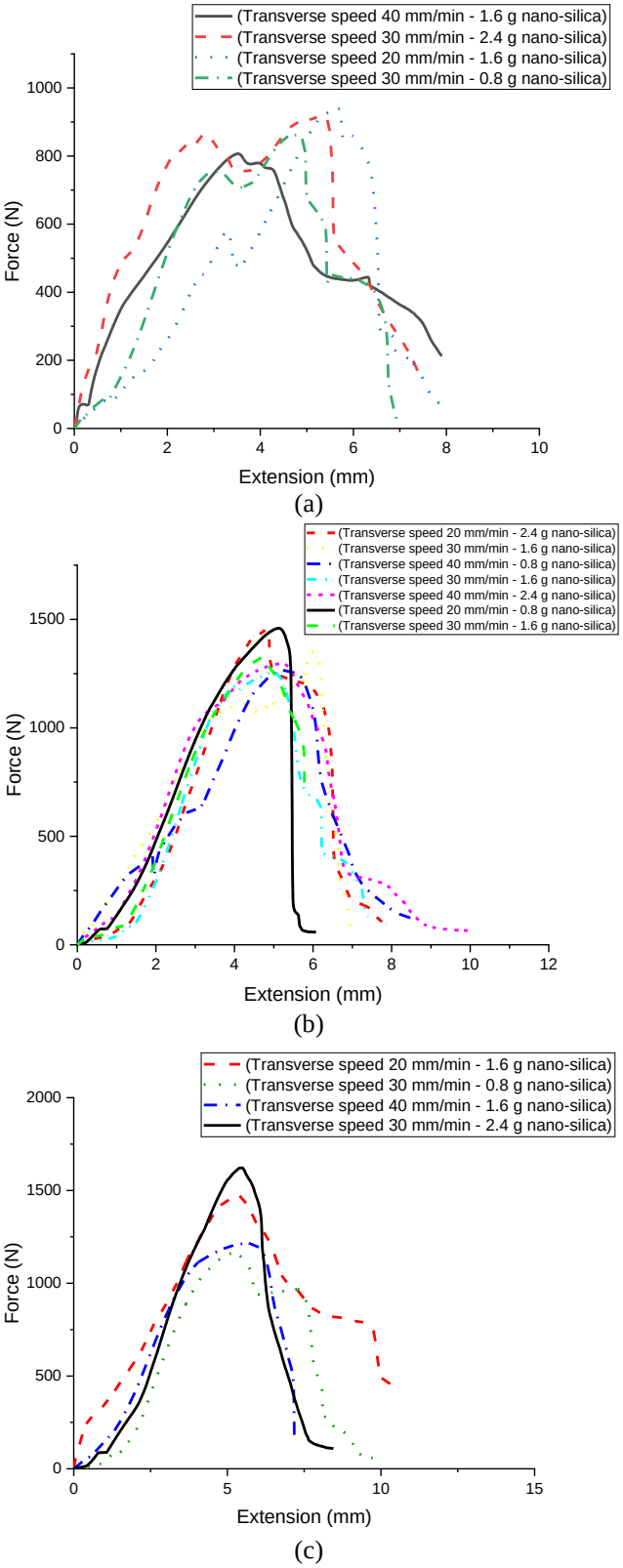

Fig. 2 The effect of nano particle and transverse speed on tensile force in (a) tool rotation speed=400 rpm, (b) tool rotation speed=600 rpm, (c) tool rotation speed=800 rpm

containing 2.4 g nano-silica shows the highest tensile strength at a transverse speed of 400 mm/min and thereby failed later as compared to other specimens. The specimens

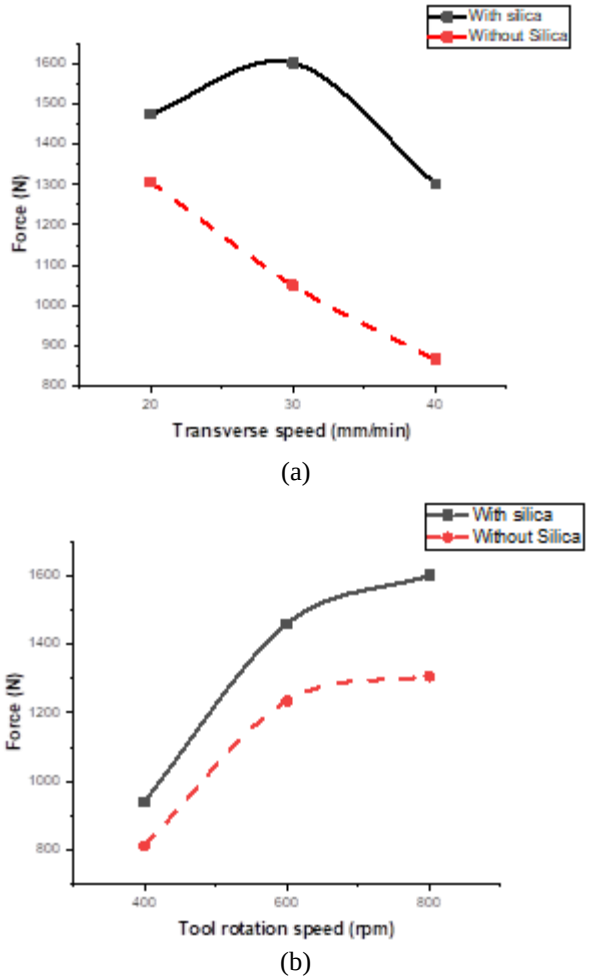

Fig. 3 Effect of process factor on tensile strength, (a) interaction of nano-silica addition and tool rotation speed, (b) interaction of nano-silica addition and transverse speed

show relatively reasonable tensile strengths at a transverse speed of 400 mm/min. The load tolerated by the specimens is decreased by increasing the transverse speed. The specimen containing 1.6 g nano-silica shows the lowest tensile strength at a transverse speed of 40 mm/min.

As seen in Fig. 2(b), the specimen reinforced with 0.8 g nano-silica shows the highest tensile strength at a transverse speed of 20 mm/s. In contrast, the specimen reinforced with 2.4 g nano-silica tolerates a tensile load close to that tolerated by the previous specimen at the same transverse speed of 20 mm/s, with the exception that the joint fails with a delay. The specimens showed a higher tensile strength at lower transverse speeds at a tool rotation speed of 600 rpm.

According to the results, the nano-silica particle causes 36% improvement in mean value of tensile strength. The highest tensile strength at a tool rotation speed of 800 rpm and a transverse speed of 30 mm/min was observed for the specimen containing 2.4 g nano-silica. The tensile strength of the joint decreases with increasing the transverse speed, but this drawback is largely eliminated by increasing the nano-silica level Fig. 2(c).

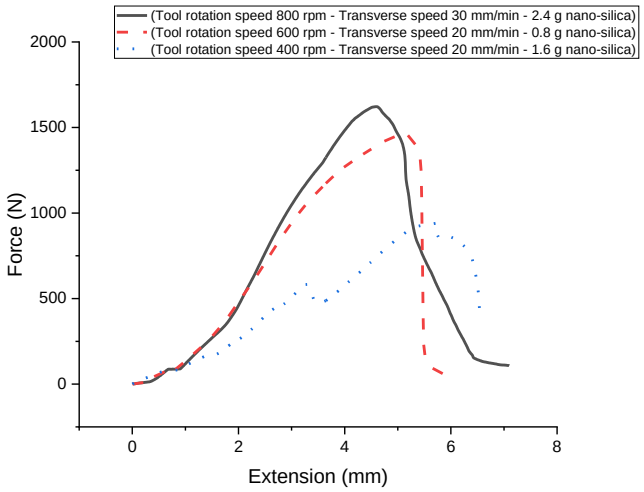

Fig. 4 The force-extension plot in optimum mode of each level

3.2 Comparison of nano-silica-reinforced and pure specimens

Fig. 3(a) compares the nano-silica-reinforced and pure specimens at different transverse speeds. By adding nano-silica at the joint, a relatively high-strength joint can be achieved even at a transverse speed of 30 mm/min. As seen, the tensile strength of pure specimens decreases with increasing the transverse speed. The reinforced specimens show the highest tensile strength up to the transverse speed of 30 mm/min, and the tensile strength of the reinforced specimens decreases with a further increase in the transverse speed. The nano-silica nanoparticles significantly improve the tensile strength of the weld joint.

Fig. 3(b) compares the nano-silica-reinforced and pure specimens at different tool rotation speeds. Fig. 3(a) shows the tensile strength increases with increasing the tool rotation speed. In general, the nano-silica-reinforced specimens show higher tensile strength than pure specimens. The tool rotation speed is directly related to the tensile strength. It is noteworthy that the tool rotation speed range used in this study is directly related to the tensile strength.

3.3 The optimal results at different tool rotation speeds

The optimal results were selected and compared to study the effect of tool rotation speed on the tensile strength Fig. 4. According to the results, the specimen containing 2.4 g nano-silica shows the highest tensile strength at the tool rotation speed of 800 rpm and the transverse speed of 30 mm/min. The lowest tensile strength is observed at the tool rotation speed of 400 rpm.

3.4 Analysis of variance (ANOVA)

The last column in Table 4 shows the probability values (P-value). A P-value of less than 0.05 indicates the significant impact of the parameter under study on the final result. In contrast, a P-value greater than 0.05 shows its insignificant impact on the final result. According to the results, the P-value for the tool rotation speed equals 0.000, indicating its significant impact on the final result. The transverse speed is ranked next with a P-value of 0.004. The results in the above table also indicate the significant but lower impact of nano-silica level than the other two parameters. On the other hand, the percentage impact of tool rotation speed, transverse speed, and nano-silica level is 118.72%, 14.82%, and 10.93%, respectively. As expected, the tool rotation speed had the greatest impact on the final results as mentioned above. The coefficient of determination (R^2-sq) is 96.37%, which seems acceptable. An R^2-sq closer to 1 indicates the greater similarity of the test results and model predictions. R-sq is calculated as follows in Eq (1):

$$R^2 - squared = 1 - [SS(Error)/(SS(total)] \quad (4)$$

3.5 Model verification

The normal probability plot of residuals are presented for the specimens reinforced with silica nanoparticles. As seen in Fig. 5, all predicted results are on the line or scattered close to the reference line. The results closer to the reference line are more acceptable. Accordingly, the results obtained from highly precise tests seem acceptable.

3.6 2D contour plots for the mutual effects of parameters

As seen in Fig. 6(a), darker regions show the highest tensile strength of the ABS T-joint. According to the diagram, the highest tensile strength is observed for the specimen containing 1.6 g nano-silica at the tool rotation speed of 600-800 rpm and the transverse speed of 20-30 mm/min. The lowest tensile strength is observed for the specimen at the tool rotation speed of 400 rpm and the transverse speed of 20 mm/min.

As seen in Fig. 6(b), the specimen reinforced with 2.4 g nano-silica shows the highest tensile strength at the transverse speed of 30 mm/min and the tool rotation speed of 650-800 rpm. The specimens show the lowest tensile strength at the tool rotation speed of 400-500 rpm, and the tensile strength increases with increasing the tool rotation speed. The increase in the tool rotation speed generates sufficient heat for changing the solid polymer to a semi-molten material. At low tool rotation speeds, adding 2.4 g nano-silica does not significantly improve the tensile strength. In contrast, it causes a reduction in the tensile strength as the silica nanoparticles are agglomerated at the rotation speed of 400 rpm, leading to a decrease in the strength of the ABS T-joint.

As seen in Fig. 6(c), the highest strength is observed for the nano-silica-reinforced specimens containing 2-2.4 g nano-silica at a transverse speed of 25-30 mm/min. The lowest strength is also observed for the specimens containing 0.8-1.6 g nano-silica at a transverse speed of 30-40 mm/min. The tensile strength is increased by increasing the nano-silica level at the tool rotation speeds of 600 and 800 rpm and decreased at the rotation speed of 400 rpm.

Table 4 ANOVA results for the experimental response at different factor levels

Source	DF	Adj SS	Adj MS	F-Value	P-Value
Model	5	764405	152881	39.73	0.000
Linear	3	555879	185293	48.16	0.000
Tool rotation Speed	1	456777	456777	118.72	0.000
Transverse Speed	1	57038	57038	14.82	0.004
Nano-silica	1	42065	42065	10.93	0.009
Square	1	170618	170618	44.34	0.000
Tool rotation Speed*Tool rotation Speed	1	170618	170618	44.34	0.000
2-Way Interaction	1	37908	37908	9.85	0.012
Tool rotation Speed*Nano-silica	1	37908	37908	9.85	0.012
Error	9	34628	3848		
Lack-of-Fit	7	29369	4196	1.60	0.438
Pure Error	2	5259	2629		
Total	14	799033			

R2-sq=96.37 %
Notes: DF=degrees of freedom; Seq SS=sequential sum of square; Adj MS=adjusted mean of square; values are statistically significant at 5% level of significance; p=a statement describing F.

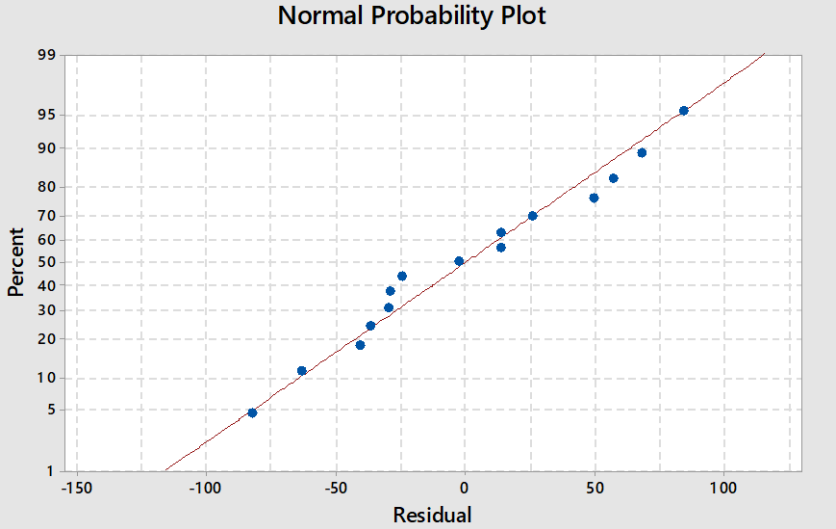

Fig. 5 Normal probability plot of SN ratio

3.7 Optimization

Fig. 7 shows the optimal FSW parameters predicted by the Box–Behnken RSM. As seen, the highest tensile strength is obtained for the specimen containing the optimal nano-silica level of 2.4 g at an optimal tool rotation speed of 755.5556 rpm and a transverse speed of 20 mm/min. The tensile strength of this specimen predicted under optimal conditions is 1627.9224 N.

4. Effect of nano-silica on the tensile strength

The tensile strength of the ABS T-joint is improved in the friction stir welding by adding silica nanoparticles. The nano-silica powder mixed with ABS acts as a filler, leading to a surface with fewer cracks and thereby a higher tensile strength. Fig. 8 displays the scanning electron microscope (SEM) image of the specimen containing 0.8 g nano-silica at a tool rotation speed of 600 rpm and a transverse speed of 20 mm/min. As seen, the silica nanoparticles added to the specimen seem insufficient for reinforcing FSW joints, and further silica nanoparticles may rehabilitate seams formed at the welding site more effectively. The nano-silica size decreases by increasing the tool rotation speed.

As seen in Fig. 9, the size of silica nanoparticles decreases from 60 nm to 20-30 nm in the specimen containing 2.4 g nano-silica at a tool rotation speed of 800 rpm. The smaller nanoparticles fill the groove at the welding site, leading to an increase in the tensile strength Fig. 10. The SEM image of the welding surface of the pure specimen (without nano-silica) shows that the seam gaps formed in this specimen caused a reduction in the tensile strength. Fig. 11 shows the SEM image of the specimen

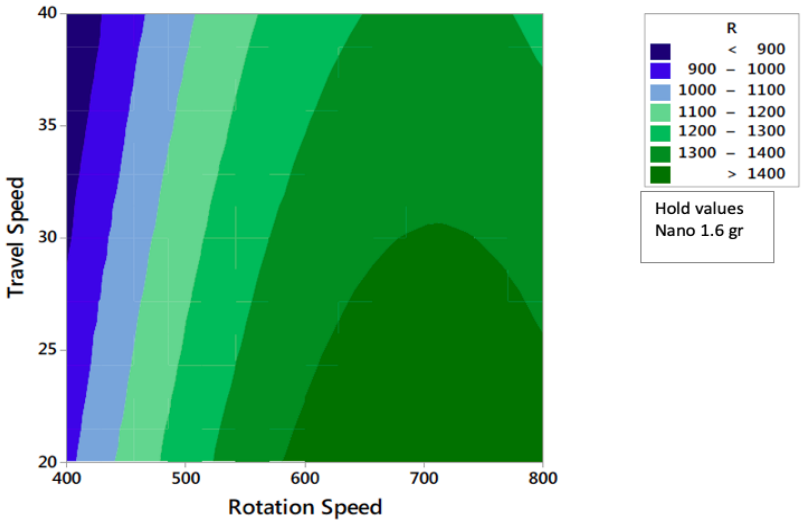

(a)

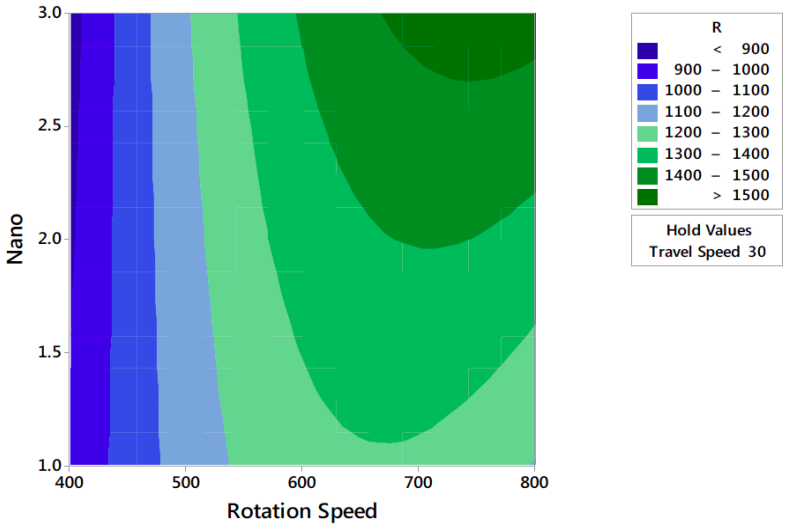

(b)

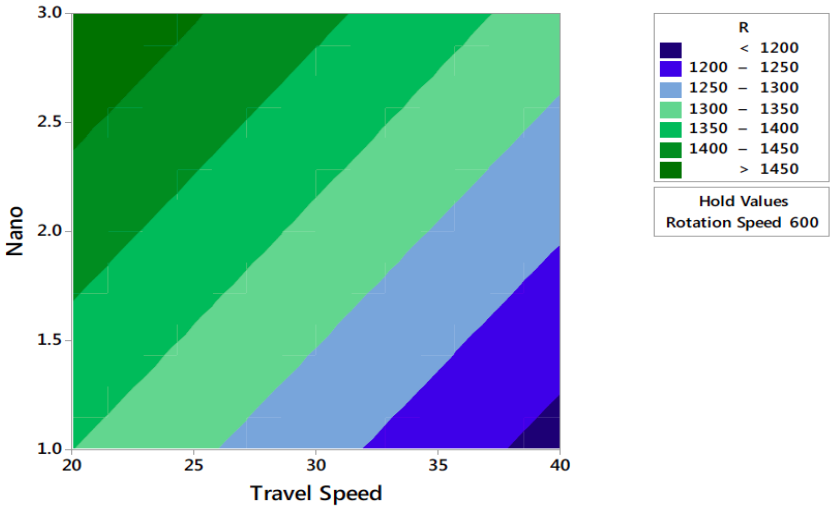

(c)

Fig. 6 2D contour plots of the response variable (tensile strength (N) for the different experimental factors (two-factor-at-a-time); (a) Tool rotation speed and transverse speed [1.8 g nano-silica], (b) Tool rotation speed and nano-silica [transverse speed=30 (mm/min)], (c) Transverse speed and nano-silica [tool rotation speed=600 rpm]

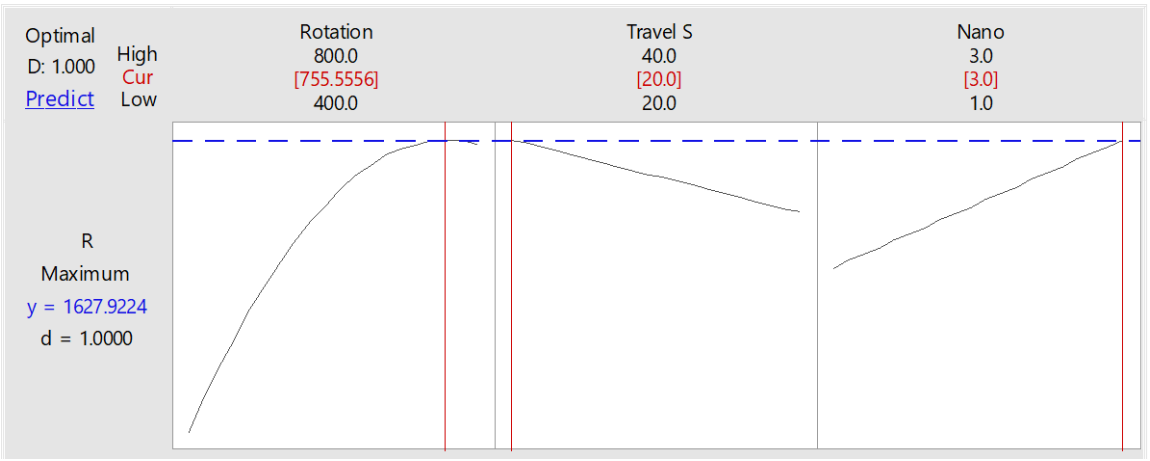

Fig. 7 optimization of process parameters

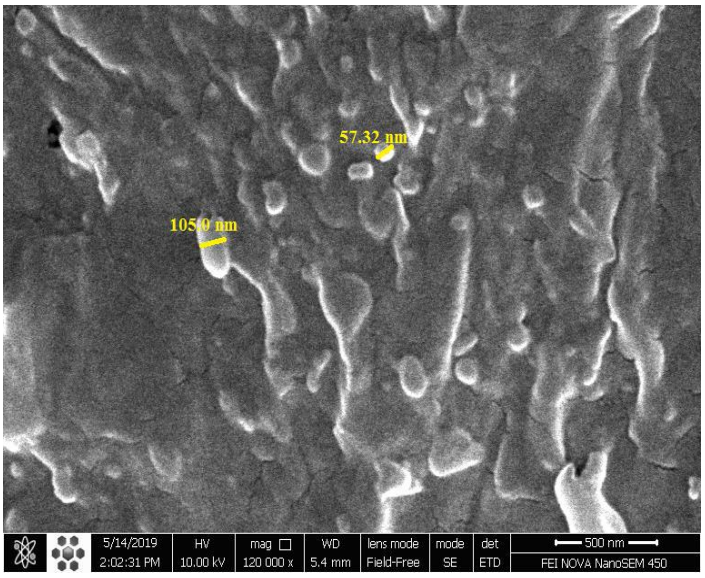

Fig. 8 SEM image from fracture surface after tensile testing for the joint fabricated by 0.8 g nano-silica

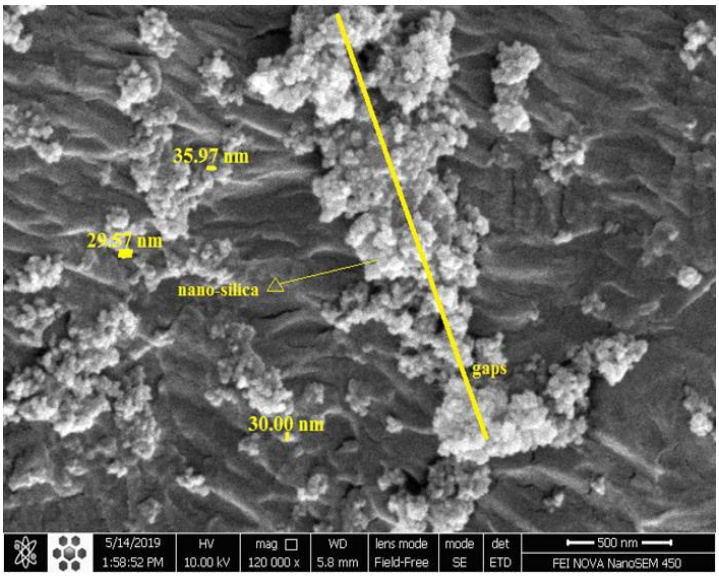

Fig. 9 SEM image from fracture surface after tensile testing for the joint fabricated with 2.4 g nano-silica and 800 rpm of tool rotation speed

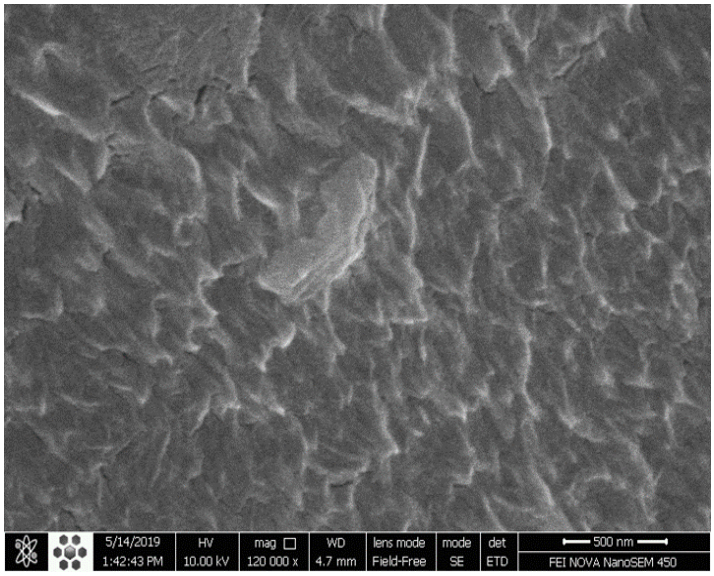

Fig. 10 SEM image from fracture surface after tensile testing for the joint fabricated pure specimens (without nano-silica)

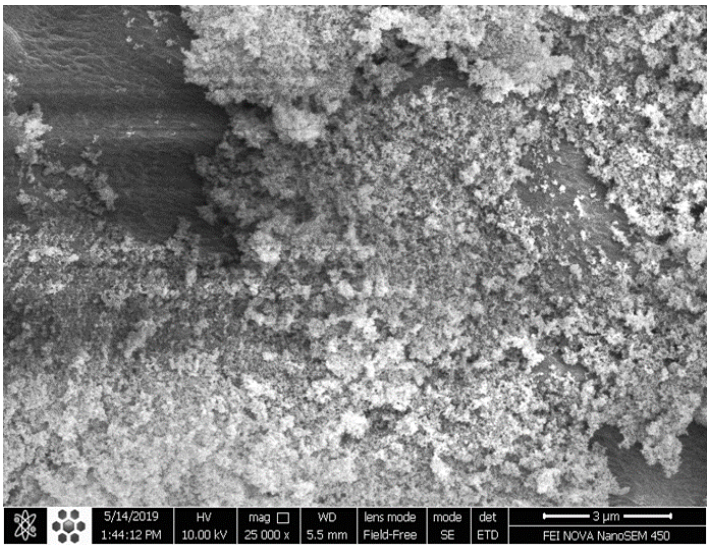

Fig. 11 SEM image from fracture surface after tensile testing for the joint fabricated with 2.4 g nano-silica and 400 rpm of tool rotation speed

containing 2.4 g nano-silica at a tool rotation speed of 400 rpm. The silica nanoparticles are accumulated in various zones, causing the formation of nanoparticle agglomerates. The silica nanoparticles improve the ABS structure and thereby the tensile strength of the ABS T-joint at a tool rotation speed of 600 to 800 rpm. In contrast, adding 2.4 g nano-silica to the polymer decreased the strength at a tool rotation speed of 400 rpm.

5. Conclusions

This paper aimed to measure the effects of nanoparticles and Friction stir welding (FSW) parameters on an ABS T-joint and observe nanoparticle performance in the welded joints. The SEM comparison of the nanoparticle-reinforced and unreinforced welded joints would effectively represent the contributions of nanoparticles and the filler and the relationship between FSW parameters and nanoparticles.

The results were obtained upon the use of nanoparticle reinforcement in order to find the optimal parameters between these range of parameters. Furthermore, the nanoparticle quantity was set based on the groove depth on the t-flange of specimens; 2.4 g of nanoparticles filled up the groove with a width of 0.5 mm and a depth of 3 mm, and higher quantity of nanoparticles could not be assumed to be effective. The groove depth and width were set based on the welding tool size; the width and depth of the groove could not be above 0.5 and 3 mm respectively, as the welding area in the FSW process should be melted and re-consolidated to form a weld.

FSW is extensively used for joining polymers in the

industry. Moreover, acrylonitrile-butadiene-styrene (ABS) is a high-strength polymer, and silica nanoparticles may reasonably reinforce polymeric materials. In this study, generally two levels of the experiment were evaluated; 9 experiments without nano-silica and 15 experiments with different levels of nano-silica. Comparison of the two experiments shows that in general, the experiments with nano have better tensile strength. Experiments with nano-silica were analyzed and optimized by response surface methodology based on the BBD method. Three variable factors of FSW considered (tool rotation speed, transverse speed, and nano-silica). Tool rotation speed and transverse speed are an essential quantity in FSW Based on different materials.

An optimal tool rotation speed of 755.555 rpm, a transverse speed of 20 mm/min, and an optimal nano-silica level of 2.4 g were obtained according to the Box–Behnken surface response methodology (RSM). According to the analysis of variance (ANOVA) in the optimization method and resulting diagrams, the tool rotation speed had the highest impact on the weld joint strength. The transverse speed and the nano-silica level were ranked next in terms of influencing the tensile strength of the welding joint. Also, the normal probability plot of residuals displayed a good dispersion of collected results, so the selected design was excellent and fit for this study. The use of nano-silica for reinforcing the ABS T-joint by friction stir welding caused a significant increase in the tensile strength of the welding joints. Silica nanoparticles improved the polymer structure by filling cracks and seams formed during friction stir welding, leading to an increase in the tensile strength. The transverse speed significantly affected the welding joint strength so that the weld quality decreased with increasing the transverse speed. This negative impact can be related to the insufficient time for changing the solid polymer to a semi-molten state for joining two ABS sheets. As mentioned, the solid polymer is turned semi-molten and then mixed where the FSW tool rotates and eventually cools down. The high transverse speeds disrupt this process and reduce the weld quality. According to the results, adding 2.4 g nano-silica at a rotation speed of 400 rpm negatively affected the tensile strength.

References

Azhiri, R.B., Mehdizad Tekiyeh, R., Zeynali, E., Ahmadnia, M. and Javidpour, F. (2018), "Measurement and evaluation of joint properties in friction stir welding of ABS sheets reinforced by nanosilica addition", *Meas. J. Int. Meas. Confederat.*, **127**, 198204. https://doi.org/10.1016/j.measurement.2018.05.005.

Gao, J., Li, C., Shilpakar, U. and Shen, Y. (2015), "Improvements of mechanical properties in dissimilar joints of HDPE and ABS via carbon nanotubes during friction stir welding process", *Mater. Des.*, **86**, 289-296. https://doi.org/10.1016/j.matdes.2015.07.095.

Kiss, Z. and Czigány, T. (2007), "Applicability of friction stir welding in polymeric materials", *Periodica Polytechnica Mech. Eng.*, **51**(1), 15-18. https://doi.org/10.3311/pp.me.2007-1.02.

Kiss, Z. and Czigány, T. (2012), "Microscopic analysis of the morphology of seams in friction stir welded polypropylene", *Exp. Polym. Lett.*, **6**(1), 54-62. https://doi.org/10.3144/expresspolymlett.2012.6.

Mäkelä, M. (2017), "Experimental design and response surface methodology in energy applications: A tutorial review", *Energy Convers. Manage.*, **151**, 630-640. https://doi.org/10.1016/j.enconman.2017.09.021.

Peng, P., Wang, K., Wang, W., Huang, L., Qiao, K. and Che, Q. (2018), "High-performance aluminium foam sandwich prepared through friction stir welding", *Mater. Lett.*, **236**, 295-298. https://doi.org/10.1016/j.matlet.2018.10.125.

Rahimipetroudi, I., Rashid, K., Yang, J. B. and Dong, S.K. (2020), "Use of response surface methodology to optimize NOx emissions and efficiency of W-type regenerative radiant tube burner under plasma-assisted combustion", *J. Clean. Prod.*, **244**, 118626. https://doi.org/10.1016/j.jclepro.2019.118626.

Myers, R.H., Montgomery, D.C. and Anderson-Cook, C.M. (2016), *Response Surface Methodology: Process and Product Optimization Using Designed Experiments*, John Wiley & Sons.

Rezgui, M.A., Ayadi, M., Cherouat, A., Hamrouni, K., Zghal, A. and Bejaoui, S. (2010), "Application of Taguchi approach to optimize friction stir welding parameters of polyethylene", *EPJ Web Conf.*, **6**, 1-8. https://doi.org/10.1051/epjconf/20100607003.

Sadeghian, N. and Besharati Givi, M.K. (2015), "Experimental optimization of the mechanical properties of friction stir welded Acrylonitrile Butadiene Styrene sheets", *Mater. Des.*, **67**, 145-153. https://doi.org/10.1016/j.matdes.2014.11.032.

Saeedy, S., Givi, M.B. and Sadeghian, N. (2010), "Design and evaluation of feasibility study of friction stir welding of thermoplastic polypropylene sheets", *Proceeding of the ICME Conference on Manufacturing Engineering*, Babol, Iran, 1-5.

Sahu, S.K., Mishra, D., Mahto, R.P., Sharma, V.M., Pal, S.K., Pal, K., Banerjee, S. and Dash, P. (2018), "Friction stir welding of polypropylene sheet", *Eng. Sci. Technol.*, **21**(2), 245-254. https://doi.org/10.1016/j.jestch.2018.03.002.

Sahu, S.K., Pal, K. and Das, S. (2020), "Parametric study on joint quality in friction stir welding of polycarbonate", *Mater. Today Proceedings*, **39**, 1275-1280. https://doi.org/10.1016/j.matpr.2020.04.218.

Squeo, E.A., Bruno, G., Guglielmotti, A. and Quadrini, F. (2009), "Friction stir welding of polyethylene sheets", *Friction Stir Weld. Polyethylene Sheets*, 241-246.

Zhai, M., Wu, C.S. and Su, H. (2020), "Influence of tool tilt angle on heat transfer and material flow in friction stir welding", *J. Manuf. Pr.*, **59**, 98-112. https://doi.org/10.1016/j.jmapro.2020.09.038.

JL